

Lawrence Berkeley National Laboratory

LBL Publications

Title

Shell-Based Support Structure for the 45 GHz ECR Ion Source MARS-D

Permalink

<https://escholarship.org/uc/item/8j65c1qs>

Journal

IEEE Transactions on Applied Superconductivity, 32(6)

ISSN

1051-8223

Authors

Juchno, M

Benitez, JY

Doyle, J

et al.

Publication Date

2022

DOI

10.1109/tasc.2022.3158375

Peer reviewed

Shell-based support structure for the 45 GHz ECR Ion Source MARS-D

M. Juchno, J. Y. Benitez, J. Doyle, A. Hodgkinson, T. Leow, L. W. Phair, D. S. Todd,
L. Wang, D. Z. Xie

Abstract—Superconducting electron cyclotron resonance ion sources (ECRISs) using NbTi coils and optimized for 28 GHz resonant heating have been successfully operated for almost two decades. Moving to higher heating frequencies requires increased magnetic fields, but traditional racetrack-and-solenoid ECRIS structures are at their limit using NbTi. Rather than moving to a superconductor untested in this field, the Mixed Axial and Radial field System (MARS) being developed at Lawrence Berkeley National Laboratory employs a novel closed-loop-coil design that more efficiently utilizes conductor fields and will allow the use of NbTi in a next-generation, 45 GHz ECRIS. This article presents the design of the shell-based support structure central to the MARS-D magnet design, as well as structural analysis of its components and optimization of pre-load parameters that will guarantee its successful operation.

Index Terms— Superconducting magnets, special coils, Minimum-B fields, ECR ion source, magnet structure

I. INTRODUCTION

THE current generation of ECR ion sources is using superconducting magnet systems that are based on the NbTi conductor technology. The limits of this conductor performance allow to reach an on-axis field of 4 T when used for building the coils based on a traditional ECRIS magnet geometry. This limits the system resonance heating frequency to about 28 GHz and in order to push that boundary, the next generation ECRIS magnets base on the same coil geometries are require to use other types of superconductor that impose new challenges on ECRIS magnet systems construction. Lawrence Berkeley National Laboratory is developing a next generation of 45 GHz ECRIS, Mixed Axial and Radial field System Demonstrator (MARS-D), which is utilizing a novel closed-loop-coil design. Its main parameters are summarized in Table I. Thanks to more efficient use of the conductor and by eliminating a complex Lorentz force distribution caused by the magnet coils cross-talk, the new magnet system will be build using the NbTi superconductor. This article presents a design of the new shall-base support structure for the MARS-D magnet and summarizes results of its optimization analysis.

This work was supported in part by the U.S. DOE, Office of Science, Office of Nuclear Physics under contract number DE-AC02-05CH11231. (*Corresponding author: Mariusz Juchno.*)

The Authors are with the Lawrence Berkeley National Laboratory, Berkeley, CA 94720, USA. (e-mail: mjuchno@lbl.gov; jybenitez@lbl.gov; jadoyle@lbl.gov; ahodgkinson@lbl.gov; tjloew@lbl.gov; lwphair@lbl.gov; dstodd@lbl.gov; liwang-lbl@lbl.gov; zqxie@lbl.gov).

Digital Object Identifier will be inserted here upon acceptance.

TABLE I
MAIN PARAMETERS OF THE MARS-D

Microwave frequency f_{rf}	45 GHz
Resonant heating field B_{ECR}	1.6 T
Injection confinement field B_{inj}	5.7 T
Extraction confinement B_{extr}	3.4 T
Radial confinement field B_{rad}	3.1 T
Stored energy E	560 kJ

II. ECR MAGNET SYSTEMS

A. Sextupole in Solenoids

One of the two presently used coil configurations is a sextupole-in-solenoids coil arrangement, which is shown on the left side of Fig. 1. The examples of existing facilities using this type of a magnet is LBNL VENUS [1] and MSU FRIB [2] while IMP FECR magnet [3] is currently being developed. This coil configuration requires fairly large solenoid coils for generating a required axial field confinement. Thanks to the sextupole coil being close to the magnet bore, the radial field component is utilized more efficiently but the complex Lorentz force distribution due to sextupole and solenoid coils cross-talk requires to use a more complex support structure. Both the VENUS and the FRIB magnet use an aluminum former, the mandrel for solenoids, as a support structure for sextupole winding and a set of pressurized bladders during the magnet assembly.

B. Solenoids in Sextupole

An example of another type of the coil configuration, solenoid-in-sextupole shown on the right side of Fig. 1, is IMP SECRAL [4]. This configuration places an arrangement of sextupole coils outside the solenoids, which minimizes the Lorentz force interactions and simplifies the fabrication. The tradeoff is a decreased radial field efficiency due to the increased inner diameter of the sextupole coil. The placement of sextupole coils allows to utilize a simpler support structure, such as an arrangement of aluminum clamping rings as used in SECRAL.

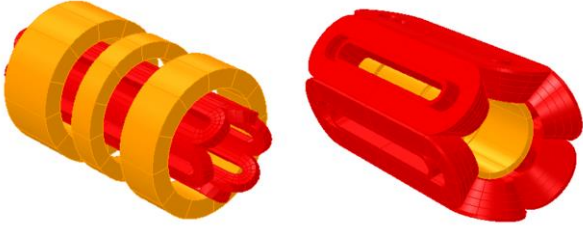


Fig. 1. Sextupole-in-solenoids (left) and solenoids-in-sextupole (right) coil configurations used in existing ECRIS magnets. Sextupole coils are shown in red while solenoids are shown in orange color.

C. Mixed radial and axial winding

Instead of a traditional arrangement of six race-track or sector coils forming the sextupole winding, MARS-D [5] utilizes a close-loop coil wound to have a hexagonal cross-section. Fig. 2 illustrates the direction and the magnitude of integrated magnetic forces acting on various parts of the MARS-D coil system. The straight bars of this winding generate the radial field component, while each end of the winding has three segments with an electric current flowing in the same azimuthal direction and thus generating a significant axial field component. An arrangement of small solenoid coils is necessary to enhance the axial field mirrors but the same azimuthal direction of the current in solenoids and the close-loop winding ends does not cause a complex Lorentz force distribution as in case of the sextupole-in-solenoid magnet. In order to maximize the efficiency of the MARS-D magnet winding, the space between the close-loop coil and segmented solenoids was minimized and therefore the solenoid former alone is not capable of supporting the close-loop coil during operation.

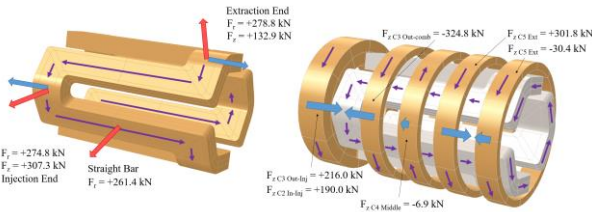


Fig. 2. Magnetic forces acting on the closed-loop winding (left) and solenoid coils (right) of the MARS-D magnet system. Radial force direction is marked in red, axial force direction is marked in blue, direction of the current is marked in purple.

III. MARS-D MAGNET SYSTEM

A. Winding and Conductor

The close-loop coil and solenoids of the MARS-D system form a very compact assembly surrounded by the radial and axial parts of the iron yoke as shown in Fig. 3. All the coils will be wound using Oxford Instruments' 6867, rectangular NbTi wires.

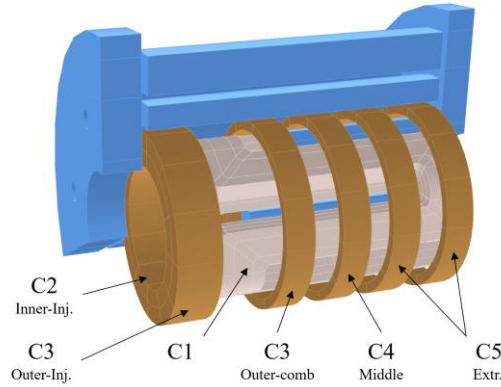


Fig. 3. Magnetic components of the MARS-D magnet system.

TABLE II
MAGNETIC PARAMETERS OF MARS-D COILS

Coil-Section	J_{eng} (A/mm ²)	I_{op} (A)	B_{cond} (T)
C1-Inner ^a	140	365.4	8.16
C1-Outer ^a	210	548.2	7.80
C2-Inner-Inj	140	365.4	8.04
C3-Outer-Inj	180	469.9	5.46
C3-Outer-Comb	180	469.9	5.95
C4-Middle	-200	521.1	5.68
C5-Extr.	180	469.9	5.94

^aThe C1 closed-loop-coil shown in Fig. 3 is wound in three layers, where the inner-most layer (C1-Inner) is powered with a lower current than the two outer layers (C1-Outer). The layers division is visible in Fig. 5.

The closed-loop coil (C1) will be wound in three layers on a removable, hexagonal mandrel to improve the manufacturability and allow for a current-graded powering of the magnet. The end-parts of the winding, which provide the solenoidal field component, will be wound with a small axial offset every two layers to minimize the magnetic field near the pole-ends. The challenges of the winding process were overcome using a local application of a glue and a conductor clamping system. The coil will be epoxy impregnated with hybrid poles made of iron and molybdenum-copper, which are optimized in terms of the radial field generation and shrinkage during the cool-down.

The solenoid mandrel made of aluminum will be shrink-fitted on the close-loop winding prior to winding the middle and the extraction solenoids (C3_{Outer-comb}, C4_{Middle}, C5_{Extr.}). The injection solenoid, made of two layers (C2_{Inner-Inj.} and C2_{Outer-Inj.}), will be wound and epoxy impregnated separately, before the final magnet assembly.

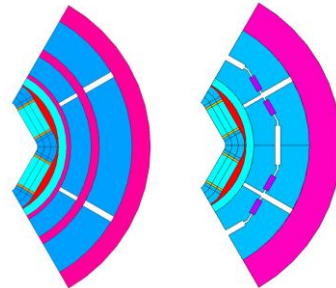


Fig. 4. Two concepts of the MARS-D support structure utilizing three layered shells (left) and bladders and key assembly (right).

B. Bladder and Key Support Structure

Due to a compact design MARS-D magnet windings and relatively thin aluminum solenoid former, an external support structure has to be used to provide coil pre-load and minimize the coil deformation during powering. Two support structures shown in Fig. 4 were considered. The selected shell-based structure designed for the MARS-D magnet is shown in Fig. 5. It utilizes a bladder and key assembly technique and supports the coil sub-assembly enclosed in a 10 mm thick protective structure made of segmented aluminum shell. The segments of the iron yoke, which are inserted between the coil sub-assembly and the external aluminum cylinder, have slotted features utilized during the bladder and key assembly operation. Axial clamp plates will be secured with six axial rods to provide structural support and axial field shielding.

The main benefit of this type of structure over the initial concept utilizing three layers of shrink-fitted aluminum cylinders is an independence of the applied pre-load from the tolerance build-up which means that all parts can be manufactured prior to the magnet assembly. As the assembly process is controlled in real-time by means of strain gauges installed on the aluminum cylinder and aluminum solenoid former, the shimming of keys that defined the pre-load can be adjusted based on the measurements. The numerical analysis showed that the by optimizing the shim thickness, the structure using the bladder and key assembly technique can provide the same pre-load level as the previous structure concept.

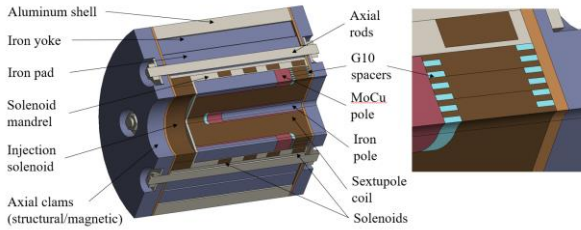


Fig. 5. MARS-D magnet support structure (left) and detailed view of the layered closed-loop coil cross-section (right).

IV. MECHANICAL ANALYSIS

A. 2D Mechanical Analysis

The initial optimization of the support structure cross-section and the coil pre-load was performed using ANSYS 2D model using a given coil geometry and a fixed outer diameter of the aluminum shell of 800 mm. The simulation was performed taking into account all main phases of the magnet life-cycle, such as the assembly utilizing bladder operation, the room-temperature pre-load, the cool-down to 4.5 K and the operation at the nominal field and current settings.

When using a 50 mm thick aluminum cylinder, the shimming of the pre-load key was set to 150 μm to guarantee that all interfaces are engaged. As the close-loop coil is enclosed in the aluminum solenoid former, the increase of the coil stress due to the room-temperature pre-load is insignificant. The main pre-load comes from the thermal shrinkage of the external aluminum cylinder and the solenoid former. As shown in

Fig. 6, the cross-section of the closed-loop coil is uniformly compressed to the level of 46-51 MPa. When magnetic forces are applied, the maximum azimuthal compression increases to 53 MPa and a uniform azimuthal stress gradient indicate no bending due to the radial force component.

The azimuthal stress distribution obtained with the 2D model was validated against the 3D model results. The result obtained from the 3D simulation shows 13 MPa lower compression in the central cross-section of the closed-loop coil. This result was expected and can be attributed to approximately +500 $\mu\text{m}/\text{m}$ of the axial strain that the conductor experiences during the cool-down that is not simulated in the plane-stress FEM simulation.

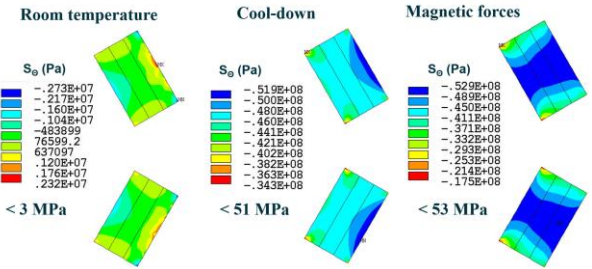


Fig. 6. Azimuthal stress in the 2D cross-section of the MARS-D closed-loop coil at each step of the magnet assembly and operation.

The results of the 2D analysis presented in Fig. 7 show a maximum stress in the aluminum solenoid former below 100 MPa but due to solenoid channels altering its cross-section, a further analysis was performed using the 3D model. At certain locations, where the hexagonal shape of the closed-loop coil limits the former thickness to 3.6 mm, the maximum stress reaches 236 MPa but it is considered acceptable for the intended aluminum alloy.

The maximum stress in the external aluminum cylinder is below 130 MPa while the stress in the radial yoke component reaches 180 MPa locally and only in the pre-load key slots.

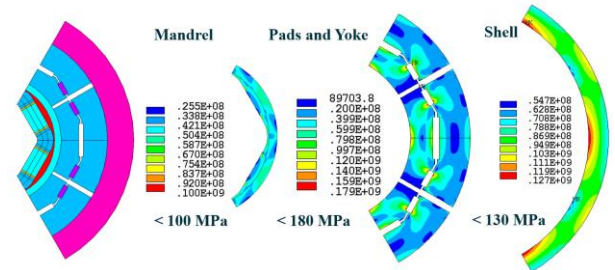


Fig. 7. Von Mises stress in the 2D cross-section of the MARS-D support structure components when the MARS-D magnet is working at the nominal field.

B. 3D Mechanical Analysis of MARS-D Windings

Due to inevitable interaction between the ECRIS magnet system coils, the 3D analysis is critical for evaluating the potential impact of the coil cross-talk on the magnet performance. Fig. 8 shows the stress distribution of the MARS-D closed-loop coil and Fig. 9 shows the hoop stress of the MARS-D solenoids.

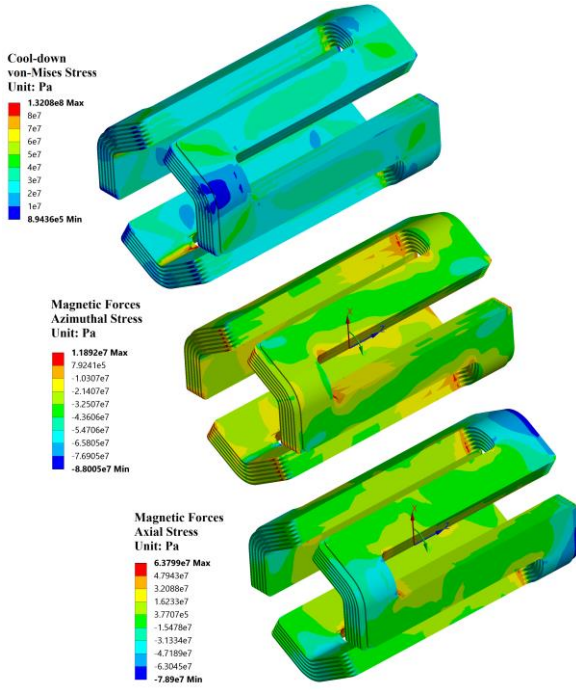


Fig. 8. Stress distribution in the MARS-D closed-loop coil. The top plot shows the von-Mises stress after cool-down, the middle plot shows the azimuthal stress due to magnetic forces and the bottom plot shows the axial stress due to magnetic forces.

The equivalent stress distribution in the closed-loop coil after cool-down (Fig. 8 on top) shows between 20 and 50 MPa stress in the majority of the coil and a local maximum of 132 MPa at the inner face of the coil where the curvature of the hexagonal shape has the smaller radius. When the magnetic forces are applied to the coil, the azimuthal stress distribution is the most relevant for the straight bars of the closed-loop coil as it provides information about potential conductor tension. The middle part of Fig. 8 shows that the sides of the straight bars remain compressed against the poles and a localized tension of below 12 MPa appears at the interface with pre-fabricated G10 spacers. The bottom part of Fig. 8 shows the axial stress distribution that is most relevant for the end-parts of the closed-loop coil. The results show ends of both sides remain compressed with the maximum compression, caused by the attracting force to the injection solenoid, is below 79 MPa.

The analysis of the hoop stress in the MARS-D magnet solenoids presented in Fig. 9 shows that the designed structure provides a rigid support for the solenoid system and prevents the radial forces acting on solenoids from developing azimuthal tension in the superconductor. The aluminum former and axial clamps maintained the segmented solenoid arrangement as well as the injection solenoid axially compressed. The low compressive stress in the injection solenoid is not considered an issue as there is no risk conductor movement or interface de-bonding.

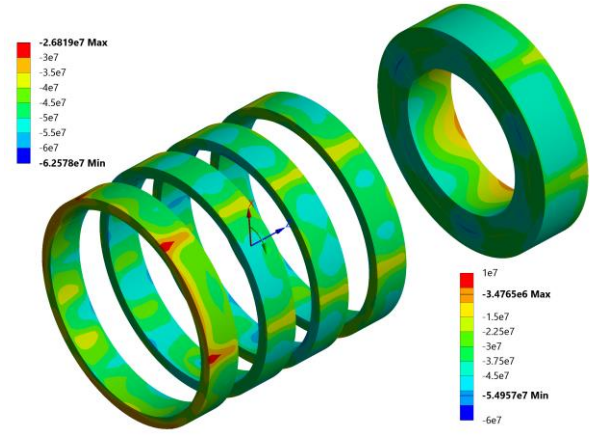


Fig. 9. The hoop stress in the MADS-D magnet solenoids. The arrangement of the middle and the extraction solenoids is shown on the left while the injection solenoid is shown on the right.

C. 3D Mechanical Analysis of MARS-D Structure

The analysis showed that the stress in components of the mechanical structure that have a continuous cross-section along the length of the magnet is close to the earlier 2D estimation. The peak stress in aluminum cylinder was 126 MPa and 236 MPa in the iron yoke. The peak stress in the shimmed keys was 342 MPa. As expected, due to a complex geometry, the 2D model did not accurately evaluate the stress in the solenoid mandrel. As shown in Fig. 10, the peak stress in the mandrel was 236 MPa.

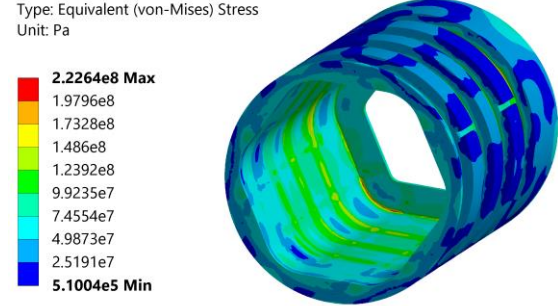


Fig. 10. The von Mises stress distribution in the solenoid mandrel.

V. CONCLUSION

The new shell-based support structure for the MARS-D magnet system was designed and optimized in terms of the coil pre-load and stress level during operation. As the closed-loop coil geometry eliminates the complex Lorentz force distribution typical for sextupole-in-solenoid coil configuration, an external shell-based structure is capable of supporting the coil enclosed inside the solenoid former without increasing the magnet complexity. Results of the analysis show that, during nominal operation, the closed-loop coil and solenoids remain well supported and the maximum conductor stress does not exceed 80 MPa.

REFERENCES

- [1] C. Taylor et al., "Magnet system for an ECR ion source," in IEEE Transactions on Applied Superconductivity, vol. 10, no. 1, pp. 224-227, March 2000, doi: 10.1109/77.828215.
- [2] H. Pan et al., "Mechanical Study of a Superconducting 28-GHz Ion Source Magnet for FRIB," in IEEE Transactions on Applied Superconductivity, vol. 29, no. 5, pp. 1-6, Aug. 2019, Art no. 4100706, doi: 10.1109/TASC.2019.2901589.
- [3] W. Wu et al., "Superconducting magnet system for HIAF," IEEE Trans. Appl. Supercond., submitted for publication.
- [4] H. W. Zhao et al., "Advanced superconducting electron cyclotron resonance ion source SECRAI: Design, construction, and the first test result," Rev. Sci. Instrum., vol. 77, 03A333, 2006.
- [5] D. Z. Xie et al., "Design of a New Superconducting Magnet System for High Strength Minimum-B Fields for ECRIS," in IEEE Transactions on Applied Superconductivity, vol. 26, no. 4, pp. 1-5, June 2016, Art no. 4100205, doi: 10.1109/TASC.2015.2511928.